

This is to certify that the

thesis entitled

A GEOCHEMICAL STUDY OF THE ROLE OF MAGMA MIXING IN THE ORIGIN OF THE MARSCOITE SUITE, ISLE OF SKYE, SCOTLAND

presented by

ELAINE KAMPMUELLER

has been accepted towards fulfillment of the requirements for

Master degree in Geology

Major professor

Date_2/16/83

O-7639

.

MSU is an Affirmative Action/Equal Opportunity Institution



RETURNING MATERIALS:
Place in book drop to

Place in book drop to remove this checkout from your record. FINES will be charged if book is returned after the date stamped below.

A GEOCHEMICAL STUDY OF THE ROLE OF MAGMA MIXING IN THE ORIGIN OF THE MARSCOITE SUITE, ISLE OF SKYE, SCOTLAND

Ву

Elaine Kampmueller

A THESIS

Submitted to
Michigan State University
in partial fulfillment of the requirements
for the degree of

MASTER OF SCIENCE

Department of Geology

1983

ABSTRACT

A GEOCHEMICAL STUDY OF THE ROLE OF MAGMA MIXING IN THE ORIGIN OF THE MARSCOITE SUITE, ISLE OF SKYE, SCOTLAND

Вy

Elaine Kampmueller

Geochemical modeling methods are applied to the Marscoite Suite using the major and trace element compositions. The REE compositions were determined by instrumental neutron activation analysis. Possible processes considered are mixing, fractionation, and combinations of the two. Models are first tested by multiple linear regression analysis of the major element compositions. If consistent with this data (r^2 values < 1.0), REE compositions are calculated using the percentages arrived at in the regressions. Agreement with the data is judged by the reproduction of the europium anomaly.

The trace element data is not consistent with any simple mixing or fractionation models for either the marscoite or the ferrodiorites. The mixing of a ferrodiorite with the Marsco epigranite and minor fractionation of plagioclase, olivine, and clinopyroxene is the model most consistent with the data.

This is dedicated to my Father the rock hound and my Mother the mountain climber

ACKNOWLEDGMENTS

I would like to thank Dr. Tom Vogel for his invaluable assistance on this project and for his patience with its progress. Dr. John Wilband deserves a word of thanks for his help in the field and on the computer. And to Sue Tituskin, Carolyn Rutland, Tom Taylor, and Steve Mattson, a thank-you for helping me to stay sane.

TABLE OF CONTENTS

LIST OF TABLES	V
LIST OF FIGURES	vi
INTRODUCTION	1
FIELD RELATIONS	3
PETROGRAPHY	6
Southern Porphyritic Epigranite	6
Felsite	6
Porphyritic and Non-Porphyritic Ferrodiorites	13
Marscoite	2 1
Marsco Epigranite	2 1
GEOCHEMISTRY	2 5
DISCUSSION	30
Origin of the Marscoite - Simple Mixing	39
Fractionation	4 5
Mixing and Fractionation	47
Origin of the Ferrodiorites - Simple Mixing	48
Fractionation	48
Mixing and Fractionation	50
Summary of Preferred Models	5 5
SUGGESTIONS FOR FURTHER RESEARCH	5 5
CONCLUSION	5 5
BIBLIOGRAPHY	57

LIST OF TABLES

Table	1:	Modes (volume %) determined by point count	2 4
Table	2:	Major element compositions (in weight percent), averages, and standard deviations. * Total Iron Fe ₂ O ₃ . I From Table 3, Thompson (1968).	a s 26
Table	3:	CIPW Norms	28
Table	4:	Comparison of major element weight percents, the study and Wager et.al. (1965).	is 33
Table	5:	Trace element compositions (REE's chondrite normalized, Ba and Sr in ppm), averages, and standard deviations. 1 From Thompson (1980).	34
Table	6:	Equations, coefficients, and r^2 values.	41

LIST OF FIGURES

Figure	1:	Geologic map of the Marsco area after Thompso (1968).	on 4
Figure	2:	Cross section of Harker's gully, Shelter Ston level (after Wager et.al., 1965). Numbers ar sample locations for this study.	
		•	5
Figure	3a:	Perthitic alkali feldspar in felsite Marl4A	7
	3b.	Detail of a (crossed nichols)	8
Figure	4a:	Perthitic feldspar with graphic texture from	
		felsite Marl (crossed nichols)	9
	4b:	Spherulitic texture in felsite (Marl4A, cross	e đ
		nichols).	10
Figure	5:	Disequilibrium features from the felsite Marl	1 F
		a. overgrowth on alkali feldspar (crossed nic	hols) 11
		b. resorbed quartz phenocryst (plane light)	12
Figure	6:	Alkali feldspar from Marl. a. potassic core	b •
		albitic rim (crossed nichols).	14
Figure	7:	a. plagioclase core b. alkali feldspar rim apatite d. quartz from the non-porphyritic	c •
		ferrodiorite Mar3 (plane light).	15
Figure	8a:	Reaction rims a. pyroxene b. hornblende from non-porphyritic ferrodiorite Mar6 (plane ligh	
	8b:	Reaction rims a. olivine (altered along fract	ures)

		<pre>b. pyroxene c. hornblende from Mar6 (plan- light).</pre>	e
			17
Figure	9:	Plagioclase ringed by mafics from the porph ferrodiorite Marl6 (plane light).	yritic
		retrodictive matro (plane light).	18
Figure	10:	Cluster of small pyroxene crystals around at alkali feldspar from the porphyritic ferrod: Mar8 (plane light).	
			19
Figure	11:	Graphic texture and feldspar from the non-porphyritic ferrodiorite Mar3 (crossed nichols).	
			20
Figure	12a,	b: Plagioclase phenocrysts from the marscot Marl2 (crossed nichols).	lte
			22
Figure	13a,	b: Twinned, zoned, and slightly resorbed plagioclases from the marscoite MarllM (crosnichols).	ssed
			23
Figure	14:	Major element variation diagrams	31
Figure	15:	Rare earth element distributions (chondrite normalized).	
		not mall sed / t	36
Figure	16:	Calculated rare earth element patterns for smixing models. Numbers refer to equations table 6.	
			44
Figure		Ce/Lu vs La/Sr	
		Ce/Lu vs Sr/Lu Ce/Lu vs Ce	46
Figure	18:	Calculated rare earth element patterns for and fractionation models in Table 6.	nixing
		and fractionation models in lable o.	49
Figure	19:	Calculated rare earth element patterns for to porphyritic ferrodiorite from mixing and	the
		fractionation models in Table 6.	51
Figure	20:	Calculated rare earth element patterns for a gabbro from models in Table 6.	the

53

INTRODUCTION

A suite of rocks exposed on the northwest side of Marsco, one of the Western Red Hills on the Isle of Skye, Scotland, has been considered a classic example of magma mixing since first described by Harker in 1904. He wrote of a hybrid rock, called marscoite, formed by the mixing of a felsite and a ferrodiorite found on either side of it. Harker's evidence for mixing consists of the occurence in the marscoite of calcic plagioclase, quartz, and orthoclase phenocrysts together in a matrix of intermediate composition. orthoclase and plagioclase phenocrysts are similar in composition to phenocrysts found in the felsite and ferrodiorite respectively. A xenolithic origin for them is indicated by disequilibrium textures such as zoning and resorption of the feldspars, mantling of the quartz by hornblende, and the coexistence of minerals (orthoclase and labradorite, olivine and quartz) which could not have crystallized simultaneously (Harker, 1904; Wager et al., 1965). The field evidence for mixing is the placement of the marscoite between the felsite and ferrodiorite with contacts between them that indicate that all three were emplaced while still hot (Harker, 1904; Wager et al., 1965; Thompson, 1968). Evidence of coexisting liquids is seen in other places within the Western Red Hills, such as between the Glamaig epigranite and the Marsco Summit gabbro (Thompson, 1968).

Major element data on the suite was added by Wager et al. (1965). Using variation diagrams (major element oxides

vs. silica) they showed that the marscoite was intermediate in composition between the felsite and the ferrodiorite.

Thompson (1968) described the suite again and accepted a mixing origin for the marscoite as he has continued to do in more recent articles (Thompson, 1980).

Magma mixing has been evaluated as a petrogenetic process by numerous studies (Donaldson and Brown, 1977; Eichelberger and Gooley, 1976; Gamble, 1979; Langmuir et al., 1978; Rhodes et al., 1980; Taylor et al., 1980; Wager et al., 1965; Thompson, 1968, 1980; Hildreth, 1981). Some of these studies have specifically investigated silic and mafic interactions. Understanding these interactions is important because of the role mafic magmas may play in the development of high-level silic magma chambers (Shaw, 1979).

The evidence cited in support of magma mixing varies widely. Eichelberger and Gooley (1976) have interpreted a mixing origin for andesites based on field relationships and the presence of xenoliths. Donaldson and Brown (1977) used volcanics with fluid inclusions to develop a mixing model for variations within oceanic basalts. Langmuir et al. (1978) applied geochemical relationships, derived from the conservative behavior of composition during mixing, to the trace element data for basalts of the Reykjanes ridge. Others (Wager et al., 1965; Rhodes et al., 1979; Taylor et al., 1980) have combined petrographic and geochemical evidence to document mixing in natural systems.

The present research will test models for the origin of

the Marscoite suite using both major and trace element geochemistry in conjunction with the petrography and field relations. Comprehensive studies that apply recent modeling methods to systems which appear to so clearly demonstrate mixing have rarely been done. Simple mixing, crystal fractionation, and combinations of the two are the processes that will be evaluated here.

FIELD RELATIONS

The Marscoite suite occurs as a narrow, discontinuous, steeply dipping sheet between the Southern Porphyritic and the Marsco epigranites of the Western Red Hills. The best exposures are found on Marsco, but it is also found on neighboring mountains. The type section is in a gully on the northwest slope named after Harker (Figures 1 and 2). Shelter Stone, a large protruding boulder, serves as a landmark. At this level, on the north side of the gully, the Southern Porphyritic Epigranite is in sharp contact with the felsite of the suite. The felsite is found injected into the granite but not chilled against it. The felsite-marscoite contact is also sharp, with cuspate boundaries. The marscoite is chilled against the felsite. A few short, thin veins of felsite invade the marscoite. After several meters the marscoite grades into a porphyritic ferrodiorite. contact between them has been observed. The ferrodiorite becomes coarser and more equigranular away from the marsoite. The ferrodiorite has a gradational contact about a meter wide with the Marsco epigranite on the south side of the gully.

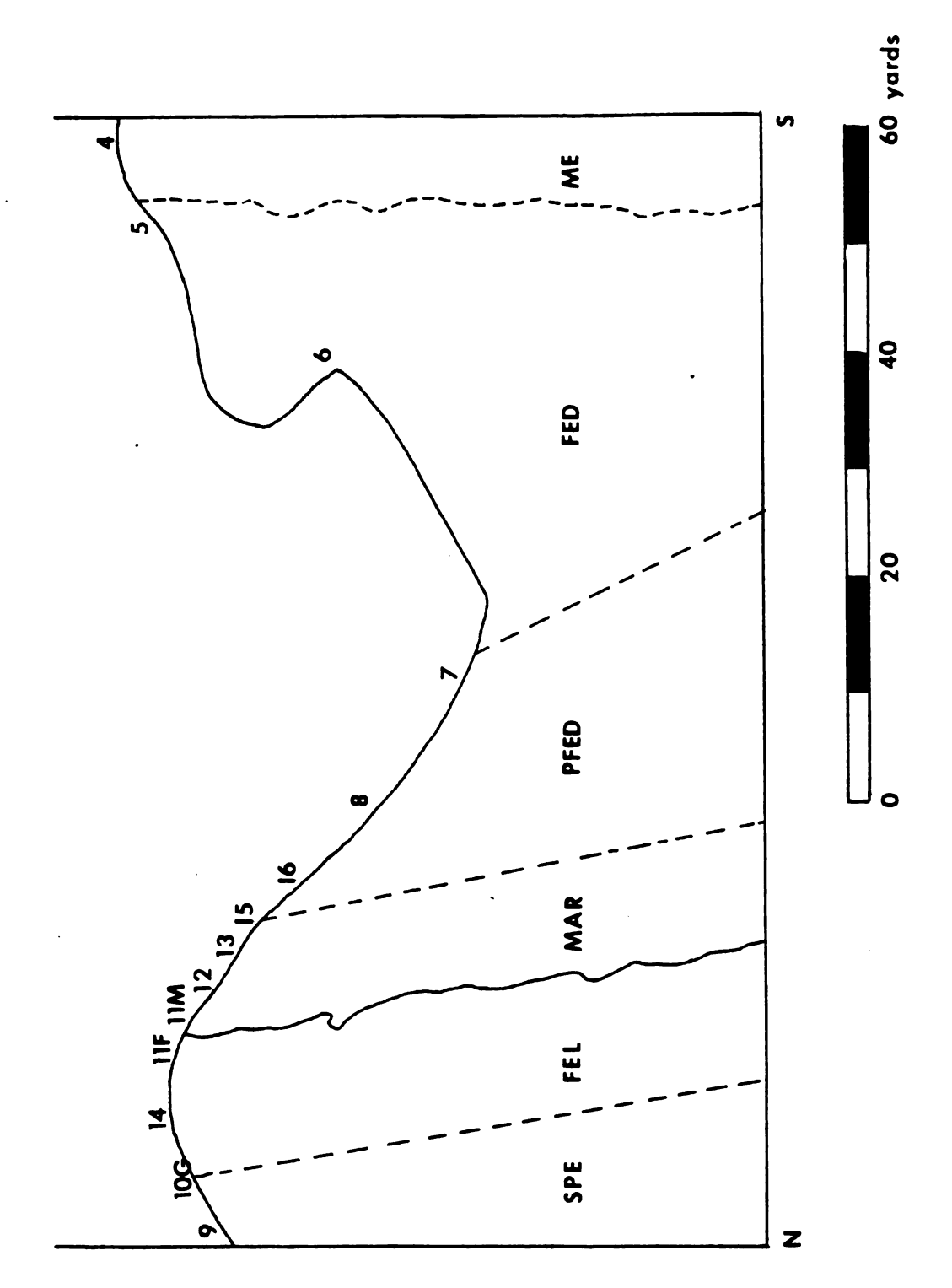
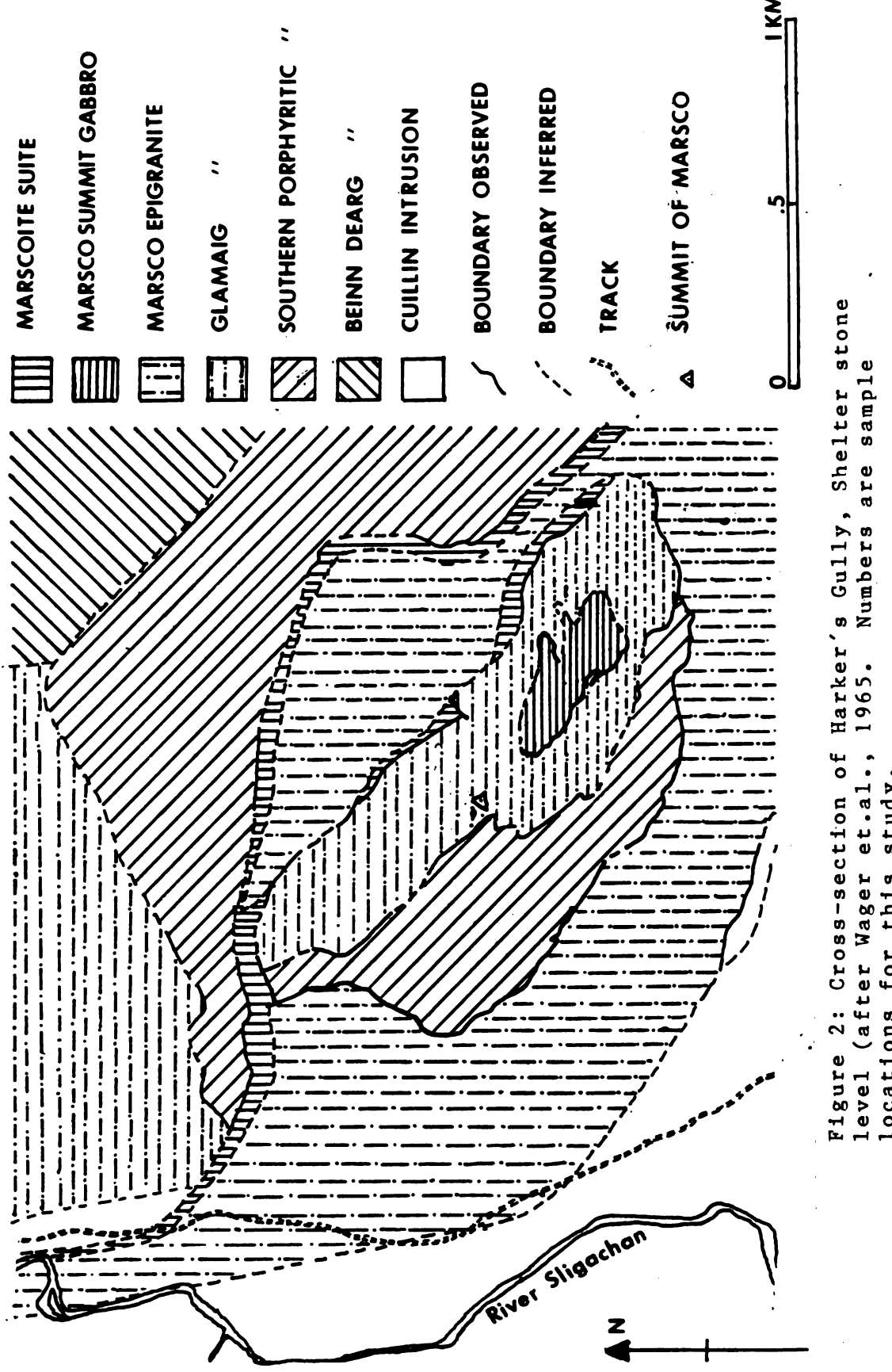


Figure 1: Geologic map of the Marsco area after Thompson (1968).



locations for this study.

The felsite, marscoite, and ferrodiorites rarely total more than 90 meters in width. Other exposures do not always contain the felsite and the marscoite occurs independently in several places. More detailed descriptions are given by Harker (1904), Wager et al. (1965), and Thompson (1968).

PETROGRAPHY

Southern Porphyritic Epigranite

This is a medium grained leucogranite. Anhedral alkali feldspar and quartz make up the majority of the rock. Alteration of the feldspars is ubiquitous and no twinning or zoning was observed. Graphic and myrmekitic textures are abundant. The few mafics which exist are opaque oxides and biotite.

Felsite

This leucogranite contains alkali feldspar and quartz phenocrysts. The feldspar compositions range from Ab₆₅Or₃₅ to Ab₃₀Or₇₀ as determined by electron microprobe analysis. They are often twinned and perthitic (Figure 3). They may be zoned with potassic rims. The matrix is fine grained and hypidiomorphic. It is composed of equal amounts of quartz and alkali feldspar with opaque oxides (magnetite or ilmenite), biotite, hornblende, pyroxene, apatite, zircon, and sphene occuring as accessories. Away from the marscoite contact graphic and spherulitic textures occur (Figure 4). Disequilibrium features were found in samples near the marscoite (Figure 5). Marl is more mafic than the other felsites. Minerals such as pyroxene, hornblende, and biotite

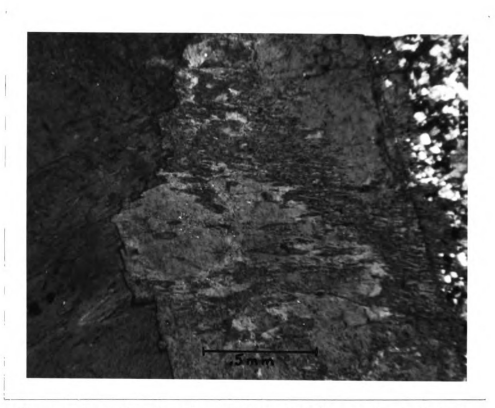


Figure 3a: Perthitic alkali feldspar in felsite $\mathtt{Marl4A}$.

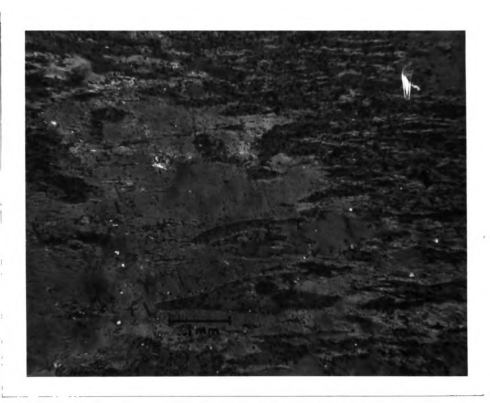


Figure 3b: Detail of a (crossed nichols).

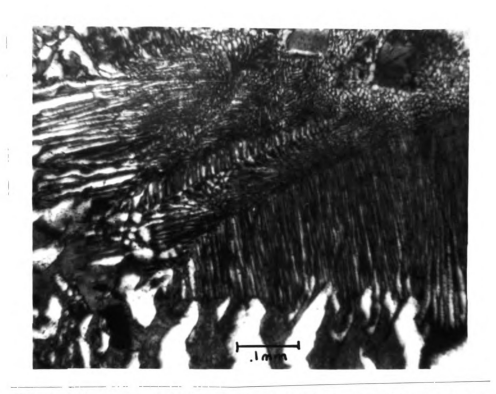


Figure 4a: Perthitic feldspar with graphic texture from felsite Marl (crossed nichols).

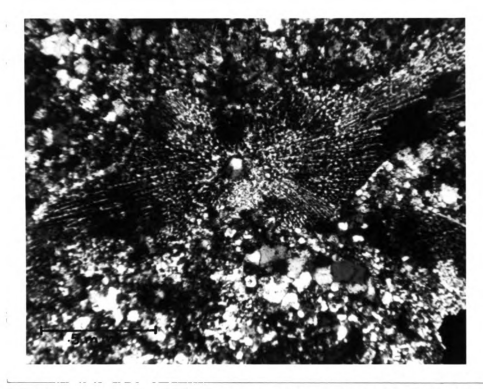


Figure 4b: Spherulitic texture in felsite (Marl4A, crossed nichols).



Figure 5: Disequilibrium features from the felsite MarllF

a. overgrowth on alkali feldspar (crossed nichols).

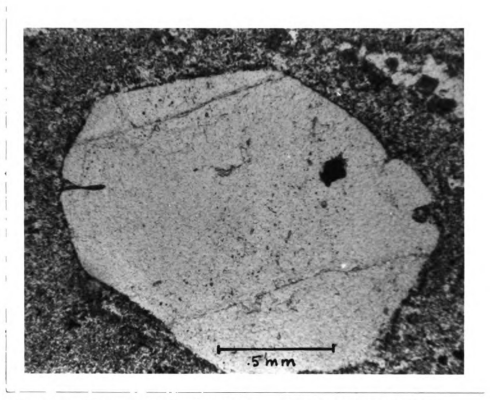


Figure 5b: resorbed quartz phenocrysts (plane light).

occur in ill-defined patches. The alkali feldspars often have potassic cores and albitic rims (Figure 6.)

Porphyritic and Non-porphyritic Ferrodiorites

The porphyritic ferrodiorite contains medium to coarse grained plagioclase phenocrysts. They comprise 5% of the Both oligoclase $(An_{13}-An_{25})$ and andesine $(An_{40}-An_{53})$ are observed. Compositions between An₂₅ and An₄₀ are rare. The phenocrysts usually occur in large, raft-like clusters but are also found separately. The crystals are rounded and often twinned and/or zoned with more albitic or potassic The plagioclase of the fine grained matrix, andesine rims. in composition, is twinned and strongly zoned. Mantles of untwinned alkali feldspar are common (Figure 7). Ortho and clinopyroxenes, such as inverted pigeonite and augite, are the most common mafic minerals. The rest of the matrix consists of hornblende, biotite, olivine (much altered to serpentine), quartz, opaque oxides, and apatite. Reaction rims between pyroxene and hornblende and clusters of mafic minerals are common (Figures 8-10). The texture of both rock types is hypidiomorphic with spherulitic and graphic patches (Figure 11). The matrix of the non-porphyritic ferrodiorite is coarser grained but otherwise identical petrographically to that of the porphyritic ferrodiorite. Very complete descriptions of both types of ferrodiorite are given by Wager and Vincent (1962) along with a discussion of the name.

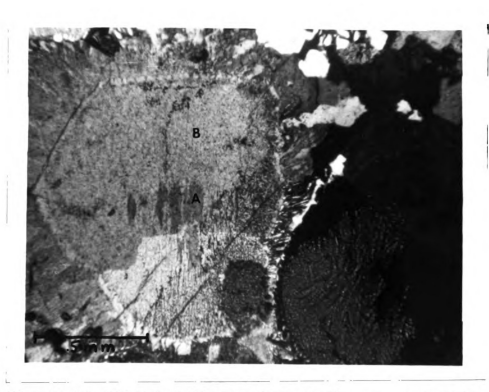


Figure 6: Alkali feldspar from Marl. a. potassic core b. albitic rim (crossed nichols).

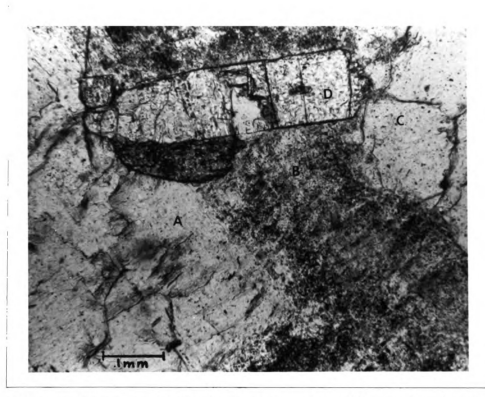


Figure 7: a. plagioclase core b. alkali feldspar rim c. apatite d. quartz from the non-porphyritic ferrodiorite Mar3 (plane light).



Figure 8a: Reaction rims a. pyroxene b. hornblende from the non-porphyritic ferrodiorite Mar6 (plane light).

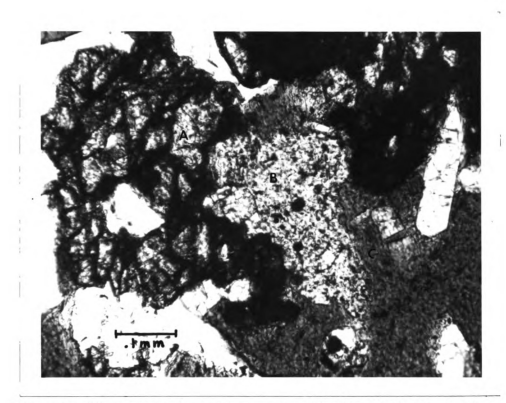


Figure 8b: Reaction rims a. olivine (altered along fractures) b. pyroxene c. hornblende from Mar6 (plane light).

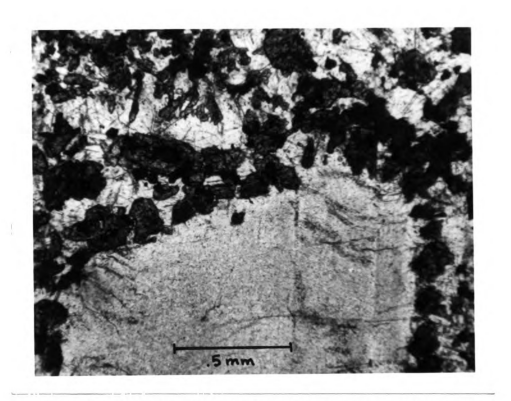


Figure 9: Plagioclase ringed by mafics from the porphyritic ferrodiorite Marl6 (plane light).

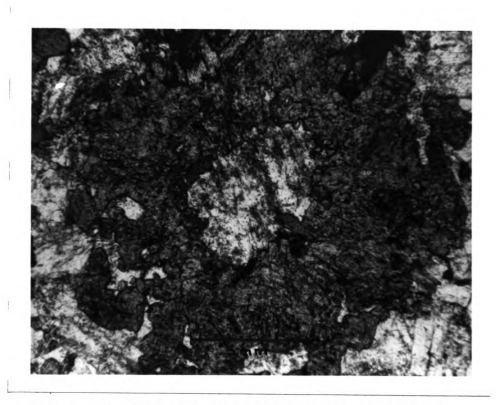


Figure 10: Cluster of small pyroxene crystals around an alkali feldspar from the porphyritic ferrodiorite Mar8 (plane light).

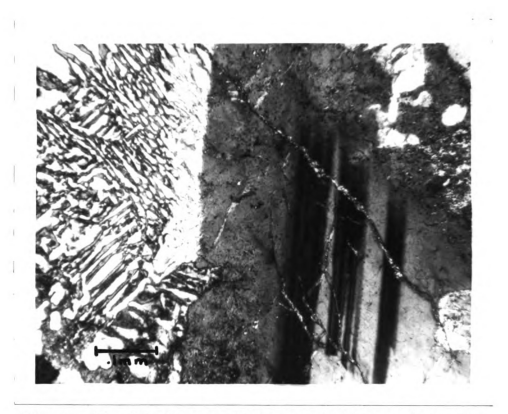


Figure 11: Graphic texture and feldspar from the non-porphyritic ferrodiorite Mar3 (crossed nichols).

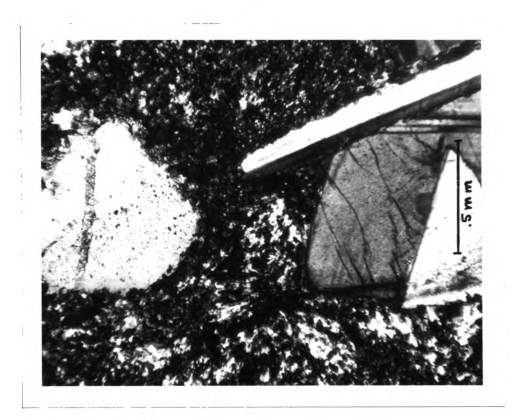
Marscoite

This intermediate rock is readily identifiable in hand sample by its porphyritic texture. Medium to coarse grained plagioclase, alkali feldspar and quartz lie in a fine grained matrix. The plagioclase phenocrysts are similar in form and composition to those of the porphritic ferrodiorite (Figures 12 and 13). The alkali feldspars (Ab₅₅Or₄₅-Ab₃₀Or₇₀) are anhedral with a patchy appearance. Some of the quartz qrains are mantled by hornblende. The fine grained, anhedral groundmass is predominantly hornblende, plagioclase, quartz, opaque oxides, and apatite. The chilled margin at the felsite contact is the only significant textural change across the outcrop.

Marsco Epigranite

The majority of this drusy granite is medium grained anhedral alkali feldspar and quartz. The feldspars are perthitic, not zoned and have been extensively seriticized. This rock is more mafic than the Southern Porphyritic epigranite or the felsite. It contains biotite, pyroxene, amphibole, opaque oxides, and a trace of olivine. Accessory minerals include plagioclase, zircon, and apatite. Graphic texture is not common.

The rock types of the suite are further described by Harker (1904), Wager et al. (1965), and Thompson (1968). Modes determined by point count in the present study (Table 1) agree well with those reported by these researchers.



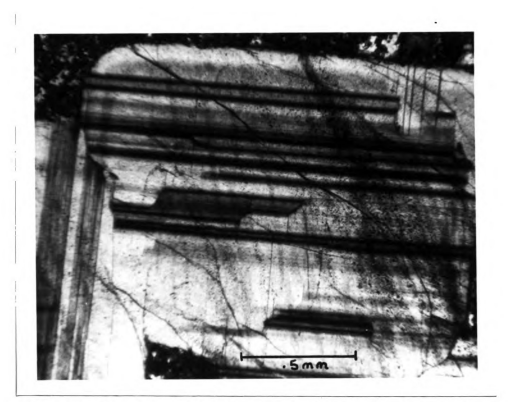
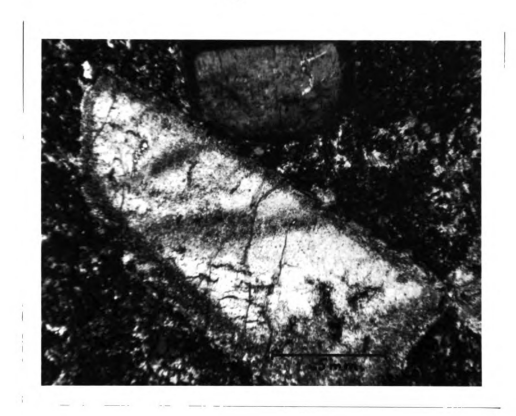


Figure 12a,b: Plagioclase phenocrysts from the marscoite Marl2 (crossed nichols).



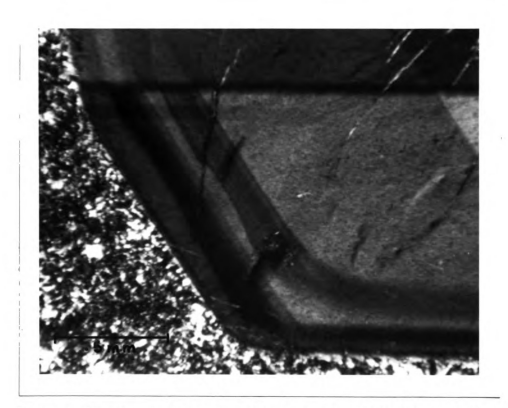


Figure 13a,b: Twinned, zoned, and slightly resorbed plagicclases from the marscoite MarllM (crossed nichols).

Table 1: Modes (volume %) determined by point count

	яе 1 s	site	Ferro		Porphyrit	1. 1.	Marscoit	oite	ME	SPE
	Marl	MarllF	dioric Mar3 Mar	v	Mar7 Mar16	עב	MarllM	Marl3		
Plagioclase	1	trace	42.0	40.1	41.3	33.1	32.7	30.2	2.4	trace
Alkali Spar	50.5	5 28.2	10.5	15.9	13.9	10.0	6.7	15.6	62.4	59.4
Quartz	17.3	3 25.1	3.5	6.5	6.5	10.3	3.0	7.7	25.0	33.8
Graphic	17.7	- '	7.4	ı	ı	,	•	1	ı	ı
intergrowth Olivine	ı	ı	3.5	2.3	5.2	4.8	ı	1	trace	ı
Pyroxene	c	c	18.5	15.4	12.8	18.3	trace	trace	1.7	ı
Hornblende	0	1.5	1.0	1.8	4.7	7.2	46.1	32.7	1.6	1
Biotite	2.4	⊲ †	4.8	9.2	5.5	5.7	trace	trace	4.2	1.5
Opaque	2.8	3.1	5.7	5.1	7.8	7.2	11.3	13.2	1.0	5.3
Oxides Serpentine Apatite	trace	e trace	trace 2.6	2.6	trace 1.9	3.5	- trace	3.4	- trace	1 1

GEOCHEMISTRY

The samples analyzed in this study were taken at the Shelter Stone level except for Marl and Mar3 which are from the Second Terrace level of Wager et al. (1965). MarllF and MarllM are from the felsite-marscoite contact. locations are shown on Figure 2. Care was taken to insure that the samples were as fresh as possible. In thin section, seriticization of the feldspars and serpentinization of the olivine is prevalent but this is not considered a limiting Pegmatitic veins are occasionally found in the area factor. and the possibility of a change in the trace element compositions must be considered. The similarity of the rare earth patterns and concentrations for samples of the same rock type indicate that such a change did not occur. Also, studies on the mobility of the rare earths during hydrothermal alteration indicates that the effect is limited to within 10 cm of the veins (Exley, 1980). It is assumed that the trace element compositions will be indicative of the petrogenetic process.

The major and selected trace element compositions of twenty samples from the Marscoite suite were determined by Barringer Magenta using inductively coupled plasma emission spectroscopy. Standard deviations of the values are based on the analyses of three sets of duplicates: Mar8A,B, Mar124A,B, Mar14A,B. The statistics and concentrations are reported in Table 2. CIPW norms are given in Table 3. The major element compositions of the rock types agree very well with those

 \sim

Table 2: Major element compositions (in weight percent), averages, and standard deviations. Total Iron as ${\rm Fe}_2{\rm O}_3$. Average from Table 3, Thompson (1968).

	3	1 2	3 6 7	, >	Aver		9	9	7 T	Aver	Mar	Mar	Mar	7
	dar 5	Maro	MaroA	E	e d		MaroA	mar/ march marcb mario ried	dar 10	7. 9	ស T T	N 7 1	Q 7 T	Mar I.
sio_2	54.2	53.0	8.67	56.5	53.40	55.8	54.5	53.40 55.8 54.5 55.2 54.7 55.05 59.3 58.2	54.7	55.05	59.3		58.9	58.0
A1203 12.6	12.6	13.6	12.3	12.9	12.85	12.5	13.2	12.85 12.5 13.2 12.9 13.2 12.95 13.3 12.9	13.2	12.95	13.3	12.3		13.0
Fe203*14.7	14.7	16.8	18.1	15.7	16.33	16.2	15.2	16.33 16.2 15.2 15.1 15.1 15.40 12.5 13.6 14.1 13.5	15.1	15.40	12.5	13.6	14.1	13.5
MgO	2.01	1.44	2.51	2.16	2.03	2.29	2.21	6 2.03 2.29 2.21 1.88 2.02 2.10 1.24 1.40 1.49 1.36	2.02	2.10	1.24	1.40	1.49	1.36
CaO	2.90	6.24	7.10	5.83	6.27	3 6.27 6.18 6.01	6.01	5.95 5.85 6.00 4.77 4.91 5.06	5.85	00.9	4.77	4.91	2.06	5.02
Na ₂ 0	3.57	4.07	3.46	3.79	3.72	3.79	3.90	3.72 3.79 3.90 3.87 4.03 3.90 4.29 3.87	4.03	3.90	4.29	3.87	4.05	3.89
K20	2.15	1.62	1.42	2.15	1.84	1.95	2.13	5 1.84 1.95 2.13 2.11 2.19 2.10 3.00 2.62 2.69 2.67	2.19	2.10	3.00	2.62	2.69	2.67
T102	2.24	2.15	2.59	2.07	2.26	2.38	2.29	2.26 2.38 2.29 2.28 2.17 2.28 1.58 1.75 1.80 1.78	2.17	2.28	1.58	1.75	1.80	1.78
P ₂ 05	0.87	0.75	1.04	0.75	0.85		0.83	0.88 0.83 0.83	0.83	0.83 0.84 0.58	0.58	0.65	0.65 0.67	0.68

Table 2 (cont'd.).

	Mar15	Aver 5 Mar	Marl	Mar Marl 11F	Mar 14A	Mar 148	Aver Fel	Mar Mar9 10G		Aver SPE	Aver Mar20 ME	Aver ME	Std. Dev.
S10 ₂	56.3	58.14	0.69		76.9	77.8 76.9 76.1 76.93 73.5 76.4 76.33 65.1 70.80	76.93	73.5	76.4	76.33	65.1	70.80	.402
A1 203	203 13.0	12.88	11.7		11.8	11.6 11.8 11.6 11.67 11.1 11.2 11.44 13.3 13.25 .221	11.67	11.1	11.2	11.44	13.3	13.25	.221
Fe ₂ 03	Fe ₂ 0 ₃ *13.6	13.46	4.44	1.64	2.28	4.44 1.64 2.28 2.24 2.05 2.58 2.85 2.82 7.65 4.73 .162	2.05	2.58	2.85	2.82	7.65	4.73	.162
MgO	1.52	1.40	0.47	0.04	0.03	0.47 0.04 0.03 0.02 0.03 0.02 0.04 0.13 0.34 0.28	0.03	0.02	0.04	0.13	0.34	0.28	.108
Ca0	5.23	2.00	1.41	0.39	0.50	1.41 0.39 0.50 0.50 0.46 0.16 0.23 0.26 2.14 1.30	0.46	0.16	0.23	0.26	2.14	1.30	.051
Na_20	4.04	4.03		3.73	3.61	3.76 3.73 3.61 3.55 3.63 3.63 3.59 3.65 4.60 4.34	3.63	3.63	3.59	3.65	4.60	4.34	.061
K20	2.53	2.70		66.4	5.48	4.37 4.99 5.48 5.46 5.31 4.86 5.04 4.79 3.83 4.22	5.31	4.86	5.04	4.79	3.83	4.22	.024
T102	1.73	1.73		0.17	0.16	0.49 0.17 0.16 0.16 0.16 0.17 0.20 0.16 0.68 0.42	0.16	0.17	0.20	0.16	0.68	0.42	.016
P_2^05	0.62	0.64	0.15	<.01	<.01	0.15 <.01 <.01 <.01 <.01 <.01 <.01 <.01 <.01	<.01	<.01	<.01	<.01	0.10	0.08	900.

Table 3: CIPW Norms

	Mar3	Mar 5	Mar6A	6A Mar6B	Mar7	Mar8A	Mar8A Mar8B Mar16	Mar16	Mar 11M	Mar 12A	Mar 12B	Marl3 Marl5	Xar.1
	3		3)) !	3	! !)) !) ! !	! !	; !)	3	1 1 1 3
0	7.08	3.31	1.83	83 6.85	6.53	4.59	6.32 4.40	4.40	8.24	10.25	8.73	9.45	6.82
0 r	13.05	9.70	∞	63 12.57 11.41 12.67 12.57 13.05 17.76 15.72 15.77 15.94 15.29	11.41	12.67	12.57	13.05	17.76	15.72	15.77	15.94	15.29
Ab	31.03	34.90	30.12	12 31.73 31.76 33.22 33.01 34.38 36.37 33.25 33.99 33.25 34.97	31.76	33.22	33.01	34.38	36.37	33.25	33.99	33.25	34.97
An	12.33	14.24	14.23	23 11.71 11.23 12.30 11.69 11.56	11.23	12.30	11.69	11.56	8.19	8.58	8.58 9.00	9.95	10.09
WO	4.97	5.08	9	38 5.04	5.61	5.12	5.26 5.11	5.11	4.90	76.7	4.83	4.47	5.14
Бn	5.14	3.63	6.43	5.32	5.65	5.54	4.72	5.07	3.09	3.54	3.68	3.42	3.87
ភ	17.21	20.15	21.54	54 18.33 18.40 17.47 17.35 17.56 14.82 16.30 16.53	18.40	17.47	17.35	17.56	14.82	16.30	16.53	16.03 16.46	16.46
Μt	2.76	3.11	3.40	40 2.84 2.93	2.93	2.79	2.78	2.78 2.78 2.29 2.52 2.55	2.29	2.52	2.55	2.49	2.54
11	4.37	4.14	2.06	3.89	4.48	4.38	4.37	4.37 4.16	3.01	3.37	3.39	3.42	3.36
Αp	2.12	1.80	2.44	1.76	2.06	1.98	1.98	1.98	1.38	1.56	1.56 1.57	1.63	1.50
D1	10.23	10.58	13.14	14 10.38 11.55		10.52	10.52 10.86 10.53		10.17 10.26 10.01	10.26	10.01	9.29	10.64
Нy	17.09	18.28	21.21	21 18.31 18.11 17.60 16.48 17.21 12.64 14.53 15.03	18.11	17.60	16.48	17.21	12.64	14.53		14.64 14.82	14.82

Table 3 (cont'd.).

	Marl	Mar 11F	Mar 14A	Mar 14B	Mar9	Mar N	Mar 20	
0	26.70	35.51	32.89	32.99	33.58	36.54	16.17	
) r	27.04	29.41	32.18	32.43	29.96	29.10	23.26	
A P	33.31	31.48	30.00	29.42	31.34	28.87	40.00	
Αn	2.24	0.17	0.0	0.0	0.0	0.0	4.45	
۸. ۱	1.69	0.71	1.00	1.01	0.32	0.44	2.42	
ᄄ	1.23	0.10	0.07	0.05	0.05	0.10	0.87	
ς. O	5.61	1.97	2.95	3.02	3.59	3.71	9.84	
/	0.85	0.30	0.26	0.07	0.18	0.15	1.44	
11	0.97	0.32	0.30	0.31	0.34	0.37	1.33	
Αp	0.37	0.02	0.02	0.02	0.03	0.02	0.24	
01	3.51	1.50	2.13	2.16	0.68	0.93	5.09	
Нy	5.01	1.28	1.90	1.92	3.28	3.31	8.04	

published by Wager et. al. (1965). See Table 4 for a comparison of the values.

Variation diagrams of the major element oxides are shown in Figure 14. ${\rm SiO}_2$ was chosen as the abcissa rather than MgO because of the wider distribution of values. The marscoites lie between the felsites and the ferrodiorites. The porphyritic ferrodiorites tend to lie toward the marscoite end of the ferrodiorite cluster. Linear trends are observed for all of the elements except ${\rm Al}_2{\rm O}_3$ and ${\rm Na}_2{\rm O}$. The changes in the values for these two elements are not large enough for distinct trends to be detected.

The rare earth elements of sixteen samples were determined at Michigan State University by instrumental neutron activation analysis using the techniques of Gordon et al. (1968) and Korotev (1976). Concentrations (Table 5) were obtained by linear regression analysis using five USGS standards activated with the samples. The chondrite normalized rare earth distributions are shown in Figure 15. Notice that the porphyritic ferrodiorites are the most primitive (lowest concentrations), with the non-porphyritic ferrodiorites and acidic rocks above the marscoites. Note also the difference in the europium anomalies; negative for the felsite and the granites, positive for the other rock types.

DISCUSSION

For a model to adequately explain the relationships between the rock types of the Marscoite suite it must be

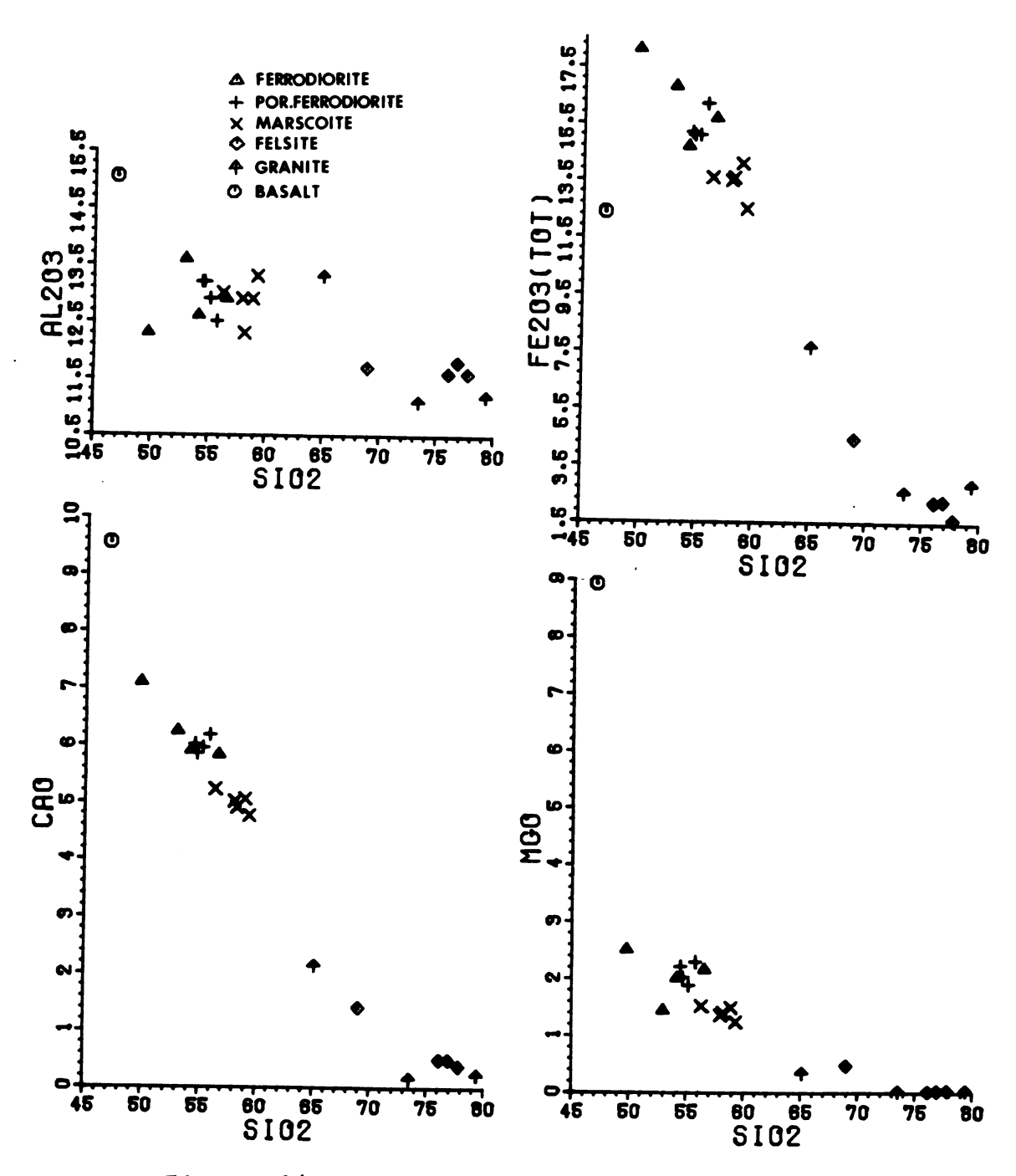


Figure 14: Major element variation diagrams

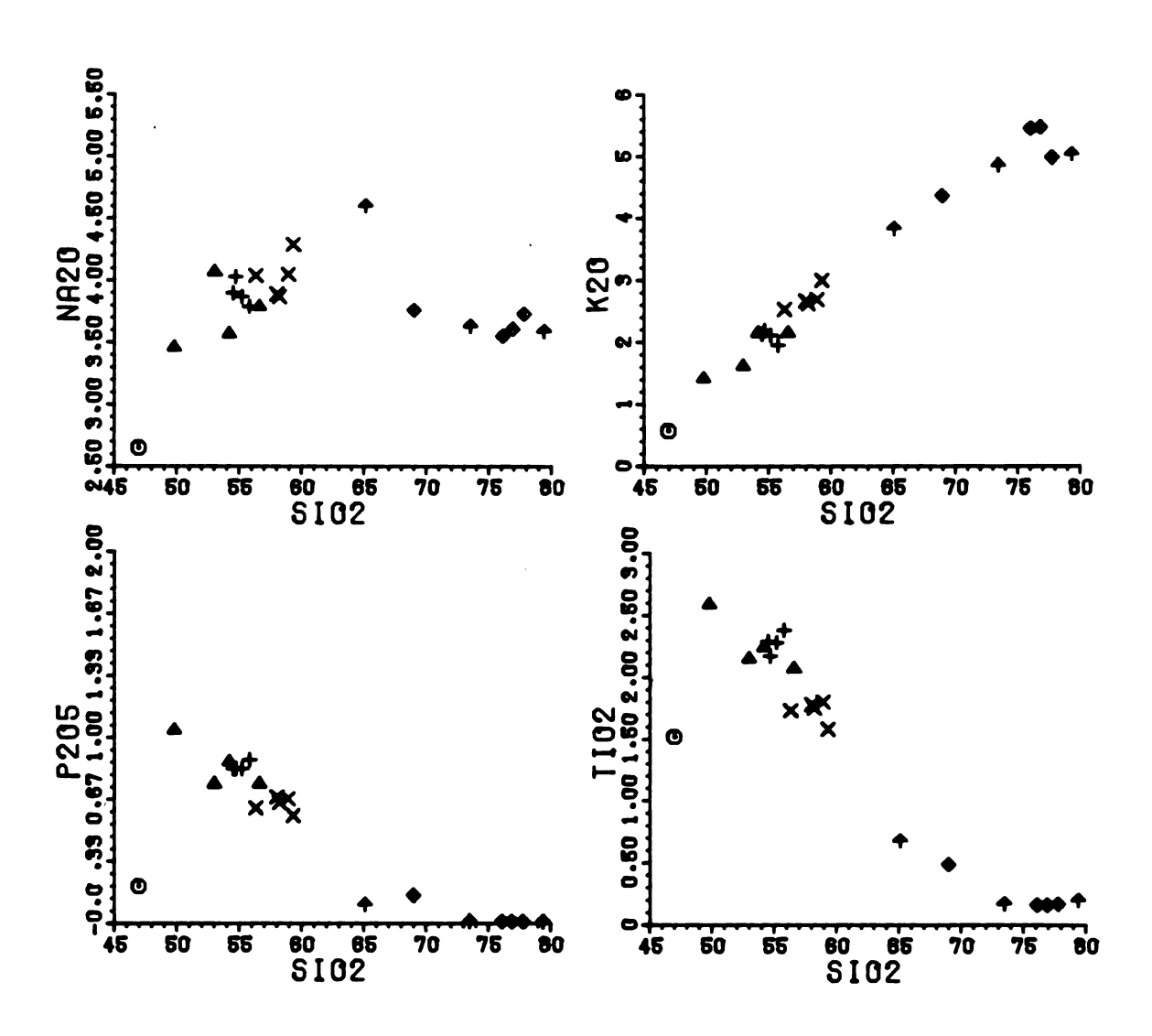


Figure 14 (cont'd.).

Table 4: Comparison of major element weight percents, this study and Wager et.al. (1965)

	Ferro	liorite	• •	ritic liorite		oite	Felsi	te	
			this	Wager	this	Wager et.al.			
sio ₂	53.40	54.18	55.05	53.43	58.14	60.07	76.93	76.41	
A1203	12.85	13.74	12.95	13.88	12.88	14.22	11.67	11.71	
Fe 203	16.33	13.87	15.40	14.73	13.46	11.09	2.05	2.53	
MgO	2.03	2.42	2.10	2.56	1.40	1.39	0.03	0.17	
CaO	6.27	6.34	6.00	6.45	5.00	4.35	0.46	0.42	
Na ₂ 0	3.72	3.46	3.90	3.69	4.03	4.02	3.63	3.62	
к ₂ 0	1.84	1.85	2.10	1.84	2.70	2.75	5.31	4.92	
TiO ₂	2.26	1.97	2.28	2.25	1.73	1.53	0.16	0.14	
P ₂ O ₅	0.85	1.30	0.84	1.10	0.64	0.60	<.01	0.04	
TOTAL	99.55	99.13	100.62	99.93	99.98	100.02	100.24	99.96	

Ba and Sr in ppm), concentrations (REE's chondrite normalized

Table	Table 5: Trace averages, and	standard standard		entratio ations.	concentrations (REE's chondrite normalized, Ba deviations.	s chon Thompso	idrite n on (1980	ormaliz).	ed, Ba	and Sr in	in ppm)
	Mar3	Mar5	Mar6A	Mar6B	Aver Fed	Mar8	Mar16	Aver Pfed	Mar 11M	Mar12	Mar13
La	105.73	153.62	122.65	117.90	124.98	94.02	103.98	00.66	117.33	115.69	112.99
C e	87.68	1111.69	100.53	98.73	99.66	78.07	78.41	78.24	94.58	91.69	90.63
Sm	71.26	83.59	87.49	67.75	77.52	55.70	60.25	57.98	63.54	70.87	71.52
Eu	74.81	89.16	82.93	72.32	79.81	73.07	72.66	72.87	74.02	82.82	78.31
Tb	61.49	75.42	89.14	75.59	75.41	58.18	60.64	59.41	54.75	68.08	56.76
Ϋ́Þ	28.07	29.20	31.59	31.42	30.07	26.93	25.00	25.97	31.73	30.93	32.42
Lu	31.33	36.14	35.33	35.28	34.52	31.38	34.45	32.92	36.23	37.46	35.10
Ва	1680	1390	1310	1650	1508	1970	2130	2050	2650	2915	2530
Sr	280	328	302	272	. 296	265	244	255	197	206	196
Ce/Lu	2.80	3.09	2.85	2.80	ı	2.49	2.28	ı	2.61	2.45	2.58
La/Sr	0.378	0.468	0.406	0.433	•	0.355	0.426	ı	0.596	0.565	0.576
Sr/Lu	8.94	9.08	8.55	7.71	ı	8.44	7.08	1	5.44	5.50	5.58

Table 5 (cont'd.).

	Mar15	Aver Mar	MarllF	Mar14A	Aver Fel	Mar9	Mar10G	Mar20	Aver Bas	Std. Dev.
La	1111.92	114.48	249.86	313.48	281.67	172.94	290.23	145.31	26.52	10.06
G e	90.05	91.74	135.00	175.80	155.40	175.23	152.10	105.13	27.63	4.20
Sm	67.27	68.30	76.69	107.40	92.05	68.83	97.22	75.64	25.03	2.06
Бu	79.75	78.73	15.56	15.35	15.46	18.77	22.79	70.26	23.61	1.71
Tb	68.91	62.13	51.65	74.10	62.88	53.07	69.29	75.49	15.57	3.28
ХЪ	27.37	30.61	54.04	69.40	61.72	65.95	73.37	54.16	9.84	1.26
Lu	34.59	35.85	40.48	50.56	45.52	49.33	51.89	47.23	8.88	0.707
Ва	2420	2629	479	427	453	141	173	2450	178	29.5
Sr	220	205	14.6	12.5	13.6	10.3	10.2	147	471	4.3
Ce/Lu	2.60	ı	3.34	3.48	1	3.55	2.93	2.23	3.11	ı
La/Sr	0.509	1	17.1	25.1	ı	16.8	25.9	0.989	0.056	1
Sr/Lu	6.36	1	0.361	0.247	ı	0.209	0.216	3.11	53.04	ı

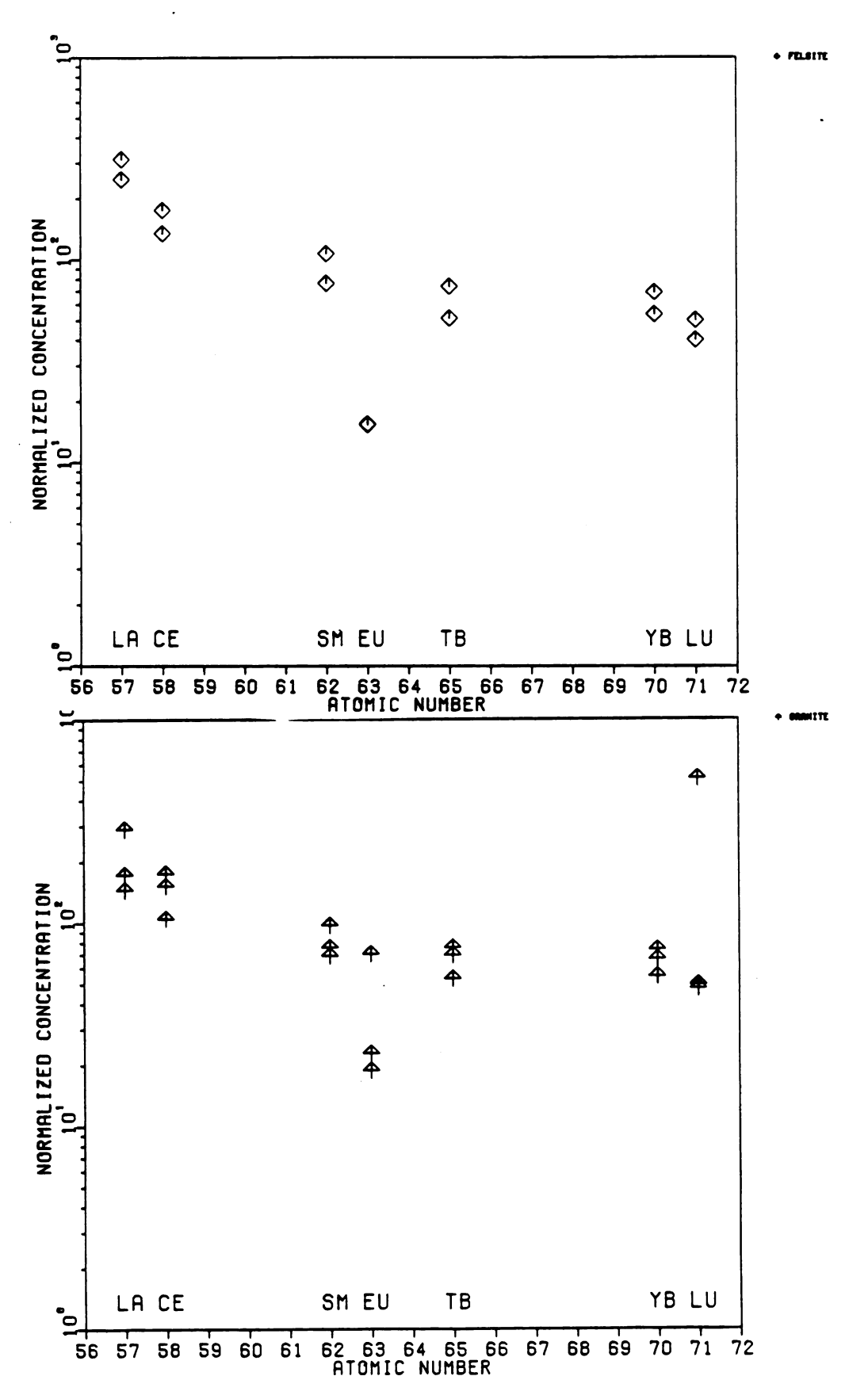
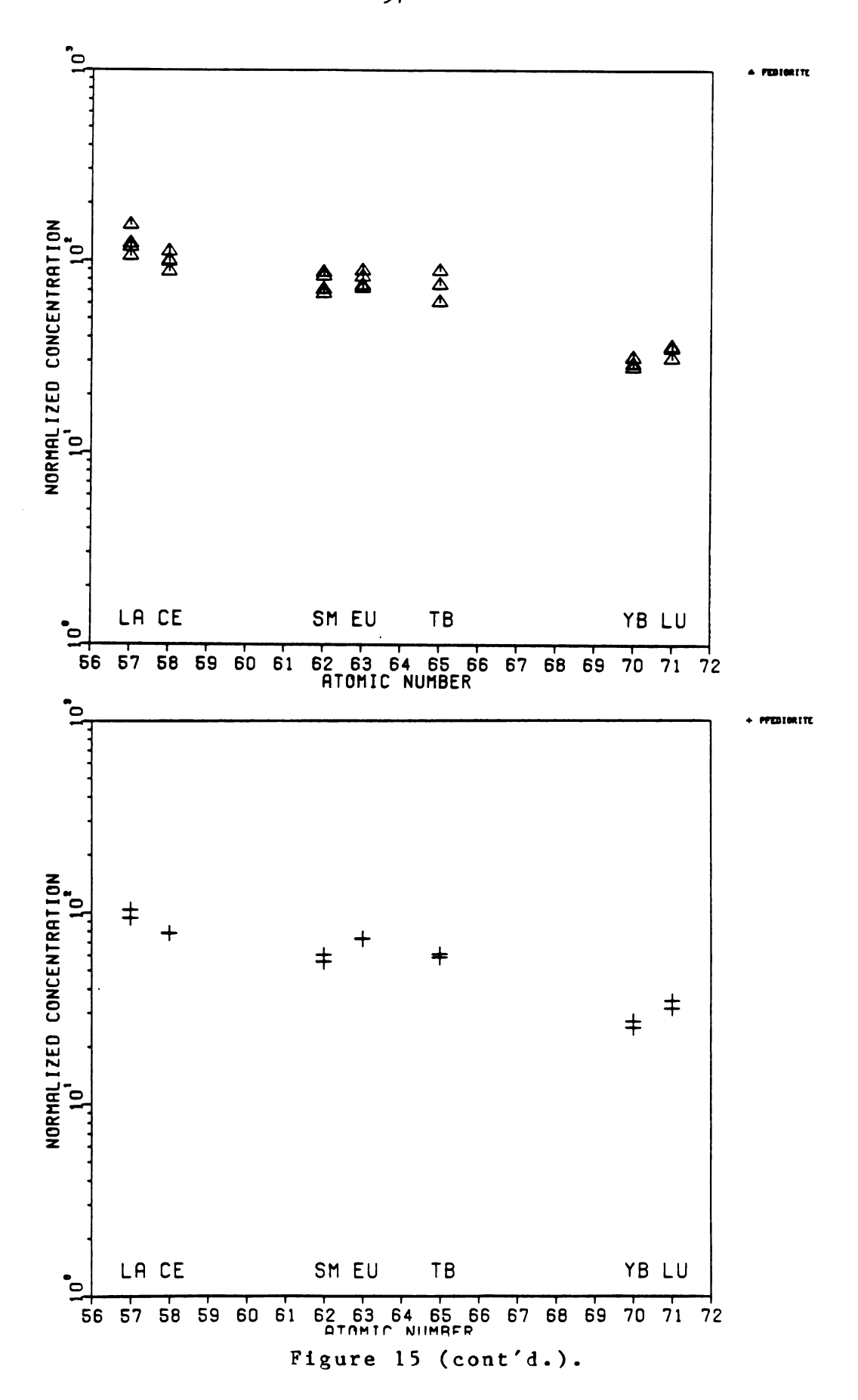


Figure 15: Rare earth element distributions (chondrite normalized)



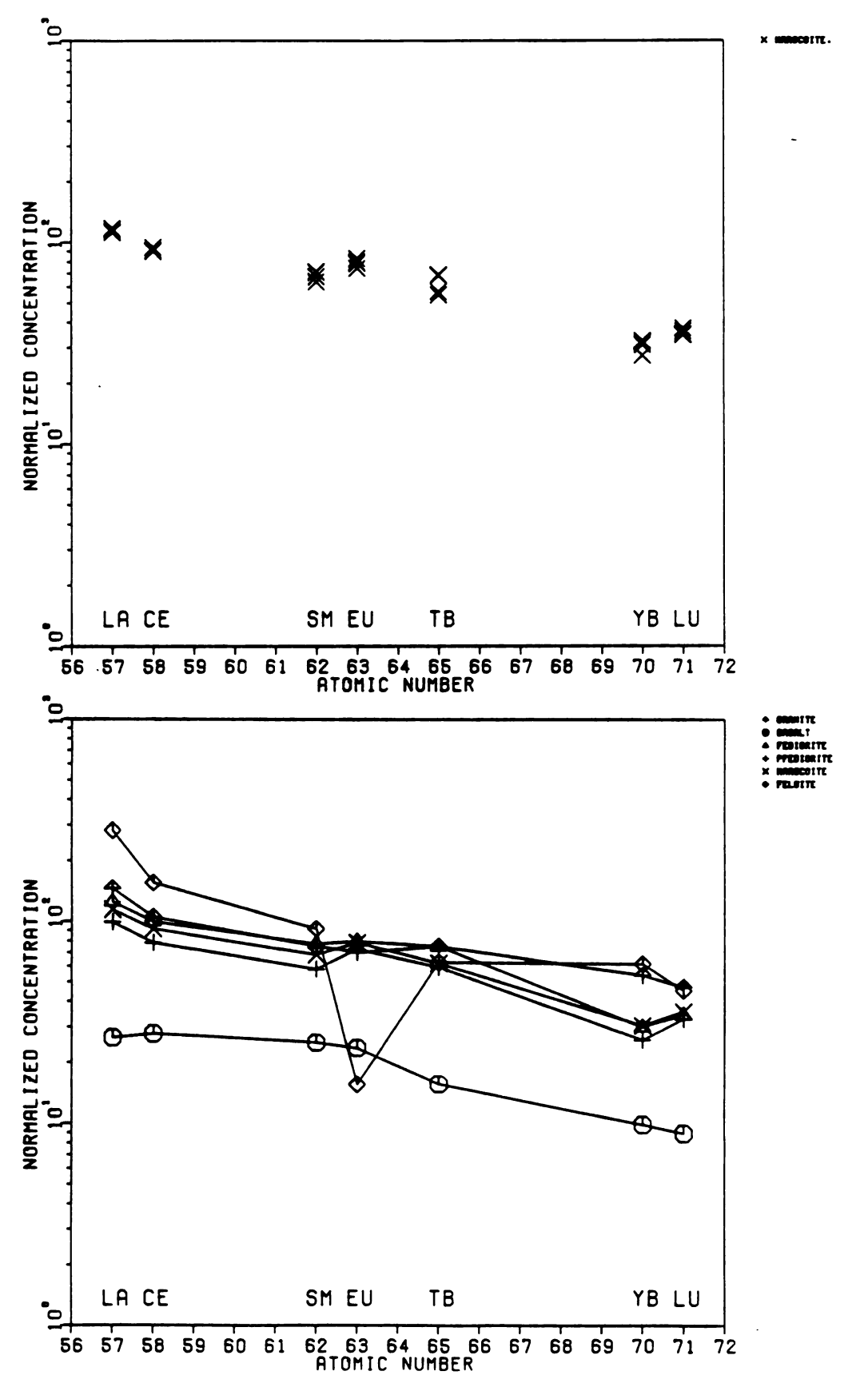


Figure 15 (cont'd.).

consistent with all of the data: field relations, petrography, and the major and trace element geochemistry. Mixing, fractionation, and combinations of the two, are processes that could provide satisfactory models. Each of these possibilities will be evaluated separately for the marscoite and the ferrodiorites. Possible parents were chosen on the basis of field relations and include rocks found in the area but not considered part of the Marscoite suite.

Origin of the Marscoite - Simple Mixing

Harker (1904), Wager et al. (1965), and Thompson (1968) have all proposed a simple mixing model for the suite. requires that the chemical composition of the daughter lie between the compositions of the parents when plotted on variation diagrams. The position of the hybrid is determined by the percentage of each parent that it contains, which should be consistent for every major and trace element. A first glance at the variation diagrams in Figure 14 shows that the rock types are in the same relative positions for each major element. Wager et al. (1965) observed the same behavior and calculated the marscoite to correspond roughly to a mixture of 26.3% felsite and 73.3% ferrodiorite. also proposed that the parents were not entirely liquid at the time of mixing because of the resorbed phenocrysts. If mixing was complete, they can be treated as liquids. mixing was incomplete, the system may show the effects of fractionation or accumulation which will be discussed later.

A more rigorous test of the mixing relationship was performed by multiple linear regression analysis (Wright and Doherty, 1970). This technique evaluates how well a linear combination of parent rocks and/or minerals expresses the chemical composition of a daughter rock. Each problem is stated by an equation. The percentages of each component which give the best approximation of the daughter are found by the least squares method. All of the variables in the equation are evaluated simultaneously and are added or subtracted to give the best fit.

Regressions were run for all possible models using the average major element composition of each rock type when more than one analysis was available. The ferrodiorites, marscoite, and felsite values are from this research (see Table 2). The Southern Porphyritic epigranite, Marsco epigranite, and Marsco Summit gabbro values are from Tables 1 and 3 of Thompson (1968). The basalt composition is sample #908 from Thompson (1972) and Thompson et al. (1980). Some of the regression equations with coefficients and the sums of the squares of the residuals (r² values) are listed in Table 6. A model was considered consistent with the major element data if the r² value was below 1.0. Below this level the individual residuals, except P₂O₅ and TiO₂, usually are within one standard deviation of the observed value.

The only simple mixing models for the marscoite consistent with the major elements are those combining either type of ferrodiorite with the felsite or Marsco epigranite.

Table 6: Equations, coefficients, and r² values

Origin of the Marscoite

Simpl	e M1	2 values
•	.7987 fed + .20216 f	7
2.	.8474 pfed + .14993 fel	.308
3	439 fed +	.138
. 4	032 pfed +	.255
5.	070 fed +	1.577
• 9	555 pfed + .1434	
7.	560 gab +	40.7
8	742 bas + .5160 m	29.8
Frac	Ţ	
9.	fed + .6072	19.508
10.	9788 pfed + .0618 p	8.56
11.	8 pfed0896 ol	3.12
12.	.157 pfed100 cpx0263 plag	9.656
13.	pfed1992 ol + .302cpx	2.51
14.	pfed0868 ol +	.308
Mixi	ing and Fractionation:	07

Mixing.	ng and Fractionation:	•
5.	.8420 fed + .203 fel0273 cpx0130 plag	.149
•	.8500 fed + .223 fel + .0371 ol08040 cpx0191 plag	.074
7.	.8040 fed + .1923 spe + .0120 plag0033 ol002 cpx	1.43
	523 fed + .2619 me00841 plag	.070
9.	.8202 pfed + .1974 me01169 plag00765 ol01185 cpx	.073
20. 1	1.2787 bas + .4340 me3856 plag18494 ol1187 cpx	.266
1. 1	1.495 gab + .3078 me4871 plag1176 ol2211 cpx	.783

Table 6 (cont'd.).

Ferrodiorites	
the	
o f	
Origin	

Star 22. 23. 24. 25. 26. 27.	<pre>ple Mixing: fed = .765bas + .2210 fel fed = .703 bas + .282 me pfed = .656 bas + .3368 me pfed = .708 gab + .265 me pfed = .92573 fed + .07919 me pfed = .94262 fed + .06028 spe pfed = .94262 fed + .06138 fel</pre>	r values 53.3 49.3 40.3 57.4 .099 .187
Frac 29. 30. 31.	ctionation: fed = 2.036 bas507 plag2874 ol148 cpx fed = 2.1136 gab6621 plag1597 ol3126 cpx pfed = 1.982 bas463 plag2769 ol129 cpx pfed = .9992 fed + .0195 plag + .0024 ol + .0024 cpx	24.74 2.57 39.15 1.898
M1x1 33. 34. 35. 37. 37. 40.	<pre>fng and Fractionation: fed = 1.7903 bas + .1843 fel5150 plag2483 ol1822 cpx fed = 1.7001 bas + .2282 me5015 plag23918 ol1592 cpx fed = 1.9869 gab + .0612 me6362 plag1496 ol2951 cpx pfed = .93433 fed + .06015 fel + .00830 plag + .00432 ol + .00121 cpx pfed = .9310 fed + .05902 spe + .00997 plag + .00371 ol + .00265 cpx pfed = .9169 fed + .07870 me + .00403 plag + .00317 ol + .00356 cpx pfed = 1.6727 bas + .2323 fel4729 plag2277 ol1714 cpx pfed = 1.5590 bas + .2884 me4558 plag21616 ol1424 cpx pfed = 1.819 gab + .1354 me5783 plag1337 ol2662 cpx</pre>	.338 .288 1.312 .066 .107 .058 .362 .277

All of the other models can be rejected as inconsistent on the basis of their high r^2 values.

If found to be in agreement with the major element data, a model can be tested for consistency with the trace element data. The REE, Ba and Sr compositions were calculated using the percentages of the parents determined by major element regression. When possible, average compositions were used in the calculations (see Table 5). It should be noted that the REE abundances of the ferrodiorites and the marscoite are very similar, usually within two standard deviations of each other. Although the differences appear to be real, they are not greatly significant. The emphasis in testing the models is on the shape of the REE pattern rather than on exact agreement between the observed and calculated compositions. The most important aspect of the pattern for this study is the magnitude and direction of the Eu anomaly.

REE patterns calculated for the simple mixing models consistent with the major element data are shown in Figure 16. The only model which reproduces the observed Eu anomaly is the mixture of porphyritic ferrodiorite and Marsco epigranite. None of the models are in agreement with the barium and strontium values.

Another test of the mixing model is done with ratio/ratio plots as used by Langmuir et al. (1978). They showed that rocks related by mixing will plot as a hyperbola when two ratios of four different elements are used. A companion plot, one of the original ratios vs the ratio of

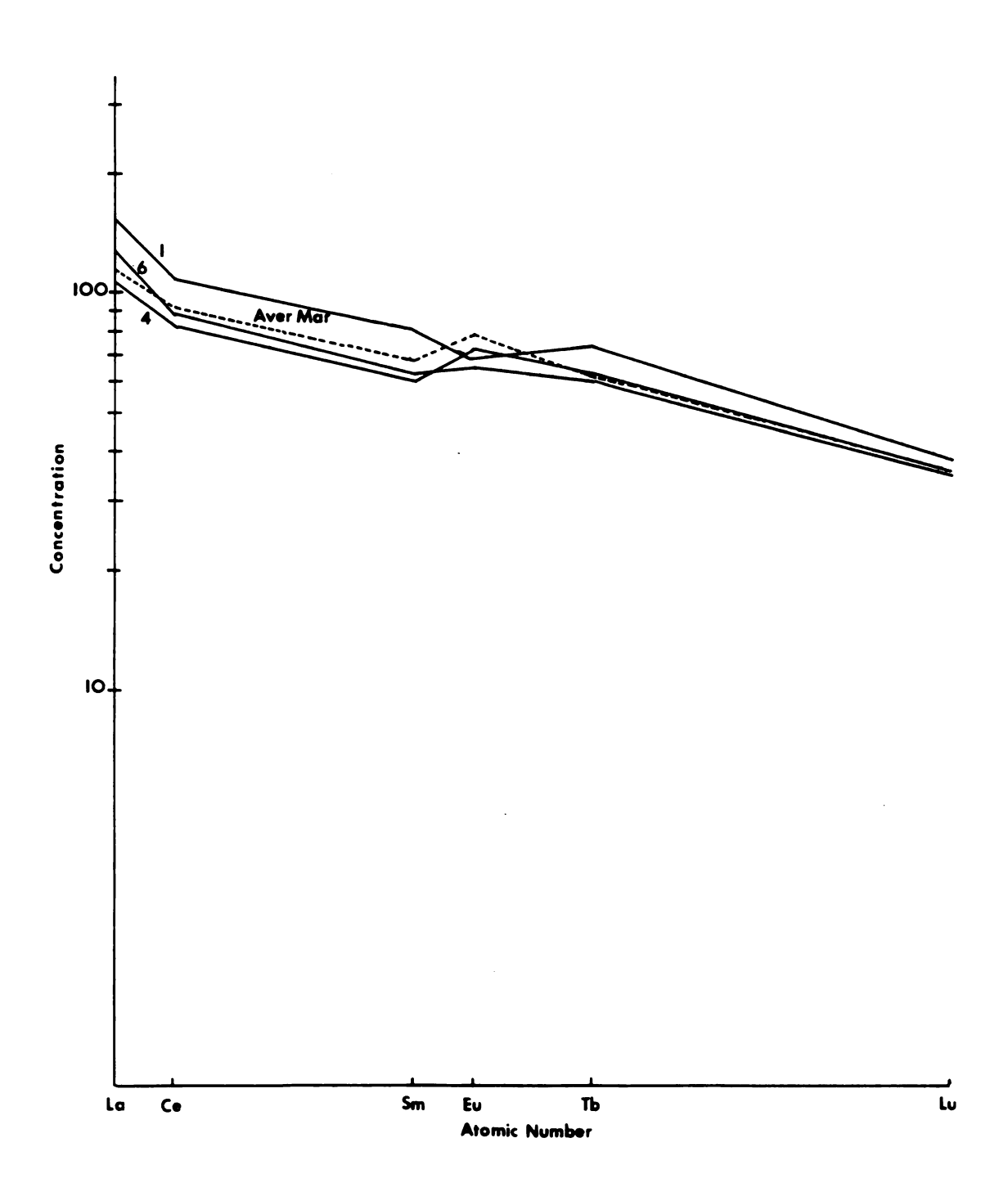


Figure 16: Calculated rare earth element patterns for simple mixing models. Numbers refer to equations in Table 6.

the denominators, should be a straight line. A pair of graphs is shown in Figure 17a,b. They seem to demonstrate mixing between the non-porphyritic ferrodiorite and the Marsco epigranite. Note that the porphyritic ferrodiorite and the felsite are not part of the trends. The ratio/element plot of Figure 17c. should also be a hyperbola. The rock types should be in the same relative positions as before, their positions being determined by the extent of mixing which is the same for all plots. For this reason also, mixing curves should be seen no matter which elements are used in the plots. No hyperbola is seen on Figure 17c. This leads to the rejection of all simple mixing models for the suite as inconsistent with the trace element data, even though the field relations, petrography, and major element compositions support them.

Fractionation

The enrichment of the REE's of the marscoite relative to the porphyritic ferrodiorite resembles a pattern that can be produced by crystal fractionation. This model is supported by the presence of phenocrysts in the ferrodiorite and similar resorbed phenocrysts in the marscoite. Major element regressions were run to test this hypothesis. Mineral compositions used in the multiple linear regression analyses are from Deer et al. (1966). They were chosen as close as possible to the compositions estimated petrographically. The only models consistent with the major element data have minerals both fractionated and accumulated (see Table 6) and

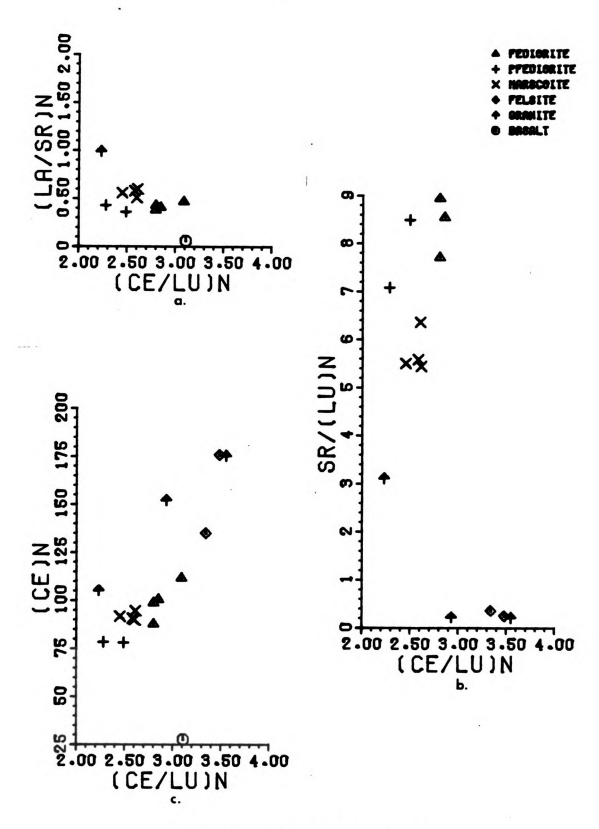


Figure 17a: Ce/Lu vs La/Sr b: Ce/Lu vs Sr/Lu c: Ce/Lu vs Ce

are combinations unlikely to occur geologically. The trace element compositions produced by fractionation are below that of the porphyritic ferrodiorite rather than above as measured. Fractionation of the felsite was rejected because it is not consistent with the petrography. Consequently, simple fractionation models are rejected because they do not explain the data.

Mixing and Fractionation

Even though simple mixing and fractionation models have been rejected individually, a combination of these processes may explain the relationships between the rock types of the Marscoite suite. As before, possible models were tested first by multiple linear regression analysis. Many models had r² values less than 1.0, some of which are listed in Table 6. Rare earth patterns and Ba and Sr compositions were calculated for these models. The mixing was computed first, then the fractionation. The Rayleigh equation for continual crystal separation (Wood and Fraser, 1976) was used. Individual partitioning coefficients were taken from Arth (1976) and bulk partitioning coefficients calculated in accordance with the relative percentages determined by regression. If the composition predicted by the mixing was above that of the marscoite the lowest coefficients were used for fractionating and the highest for accumulation. reversed if the predicted compositon was below that of the The net results of the calculations can then be marscoite. considered limiting amounts of enrichment or depletion.

shown in Figure 18. As in the simple mixing case, most models fail to reproduce the Eu anomaly observed in the marscoite. The best fit is obtained by a mixture of the porphyritic ferrodiorite and the Marsco epigranite with fractionation of plagioclase, olivine, and clinopyroxene. The improvement over the simple mixing case is a more exact reproduction of the magnitude of the Eu anomaly, a slight enrichment of the LREE's and Ba and Sr values closer to the measured values. The total amount of fractionation is approximately 2% which has very little effect on elements with partitioning coefficients less than 0.1 for the minerals involved, such as the HREE's.

Origin of the Ferrodiorites - Simple Mixing

Mixing models were tested for both types of ferrodiorite by multiple linear regression analysis (Table 6). None of these models were consistent with the major element data for the non-porphyritic ferrodiorite. The major element data for the porphyritic ferrodiorite is in agreement with combinations of the other ferrodiorite and any acidic parent. However, the REE compositions predicted by the models are all higher than the observed composition with Eu anomalies of the wrong size. Thus, none of the ferrodiorites are a result of simple mixing.

Fractionation

As in the simple mixing case, no fractionation models for the non-porphyritic ferrodiorite are consistent with the

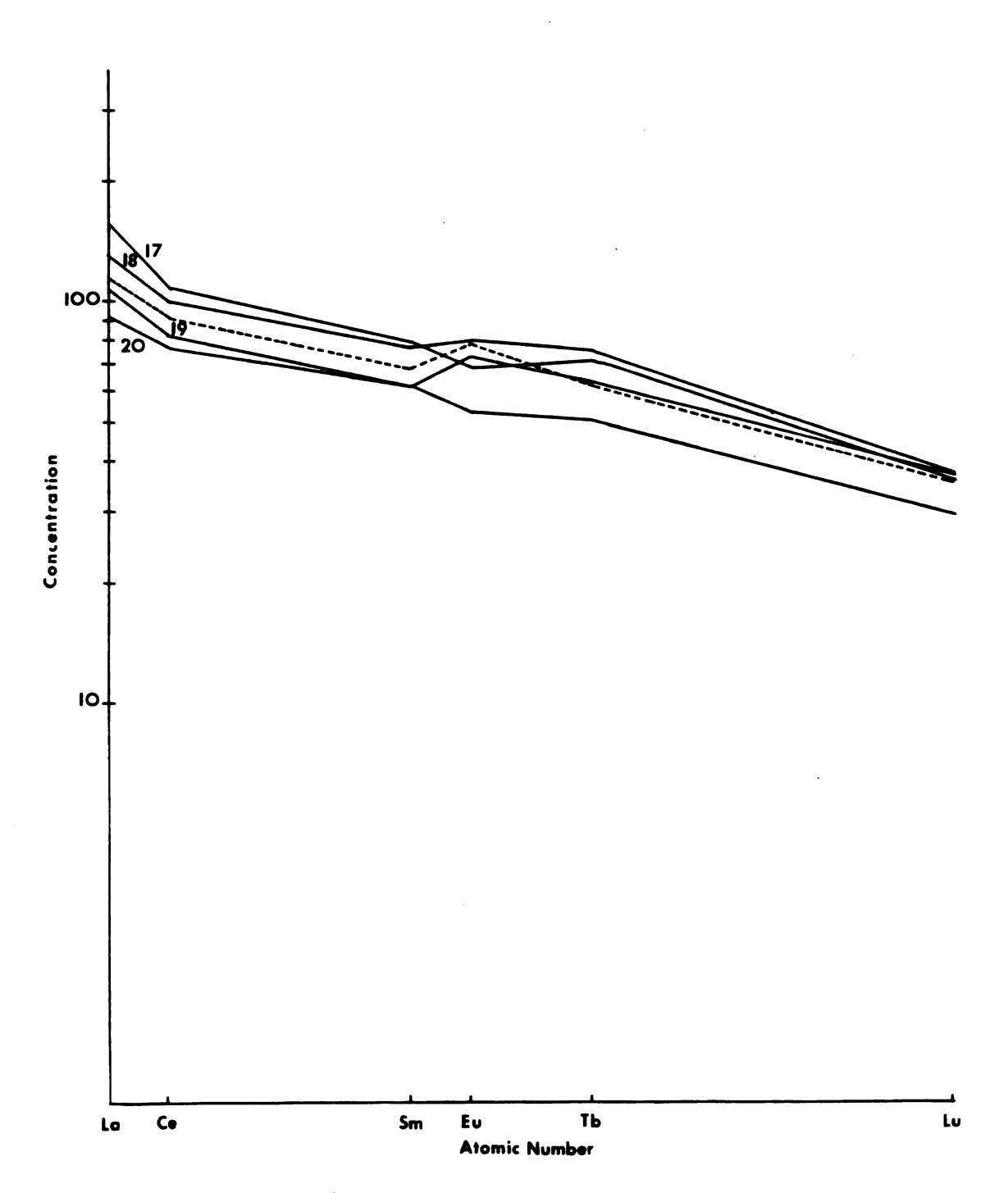


Figure 18: Calculated rare earth element patterns for mixing and fractionation models in Table 6.

major element data and only those including this ferrodiorite are consistent for the porphyritic ferrodiorite (see Table 6). Note that these models accumulate minerals instead of separating them. The calculated REE compositions are again higher than the observed ones with small positive Eu anomalies. The predicted strontium and barium values also move in the wrong directions. Fractionation alone is not the process that relates these rock types.

Mixing and Fractionation

Major element regressions were again run on possible models (Table 6). As before, the porphyritic ferrodiorite data is consistent with models involving the non-porphyritic ferrodiorite and any of the acidic parents. Models combining the basalt with the felsite or Marsco epigranite and all three minerals are also consistent with the data. As in the fractionation models, the minerals are acumulated. Patterns calculated for these models are shown in Figure 19. All of them predict either a negative Eu anomaly or a positive anomaly much smaller than the one observed. The barium and strontium values are also not sufficiently explained.

Only three models were consistent with the non-porphyritic ferrodiorite major element data. They are listed in Table 6. Both basalt models resulted in low REE patterns with negative Eu anomalies.

The trace element composition of the Marsco Summit

Gabbro was not available, so the calculations were done in

reverse for three models, one each for the marscoite and the

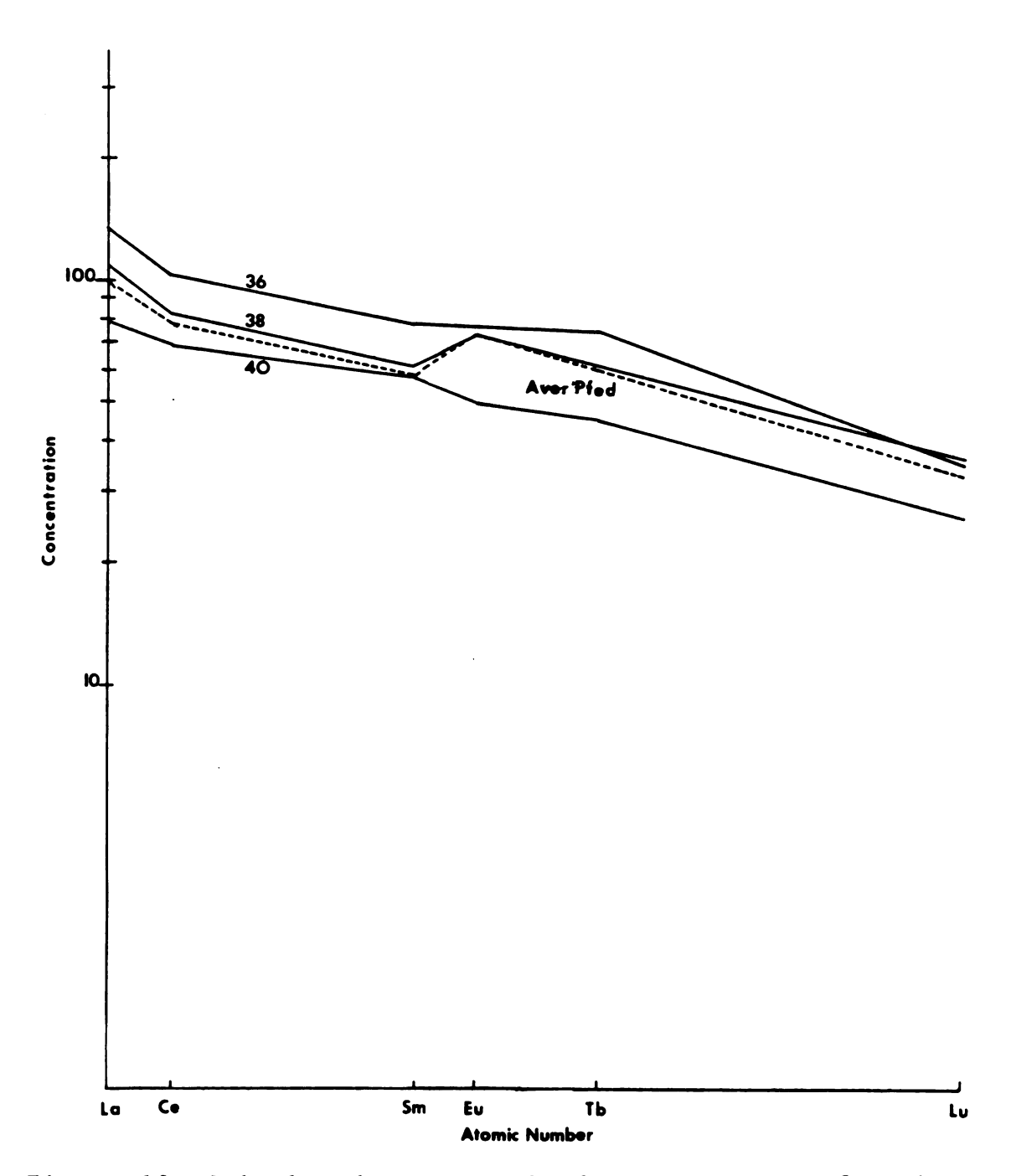


Figure 19: Calculated rare earth element patterns for the porphyritic ferrodiorite from mixing and fractionation models in Table 6.

two types of ferrodiorite. The predicted compositions for the three models had similar REE patterns (Figure 20) but widely different Ba and Sr values. Thus the gabbro was not the parent of all three rock types. A comparison of the predicted values with actual values will allow a judgment on the involvement of the gabbro in the origin of any one of the rock types.

Although no model is in agreement with all the data for the porphyritic ferrodiorite, a mixture of non-porphyritic ferrodiorite and the Marsco epigranite with an accumulation of plagioclase, olivine, and clinopyroxene is the most consistent. The major problem with this model is that the amount of accumulation is not enough to raise the Eu concentration while lowering the rest. This may be because of the mineral compositions used in the regressions or because the partitioning coefficients used in the calculations do not accurately reflect those that actually occurred. It is possible, for example, that a minor amount of potassic feldspar may have accumulated which would enrich the barium as needed, but also strontium which should be depleted. If this model is accepted for the porphyritic ferrodiorite it must also be accepted for the marscoite because the discrepancies are similar in that case.

Fewer discrepancies exist for the marscoite model involving fractionation of a porphyritic ferrodiorite and Marsco epigranite mixture. Only P, Ti, Ba, Sr and Eu are predicted more than two standard deviations from the measured

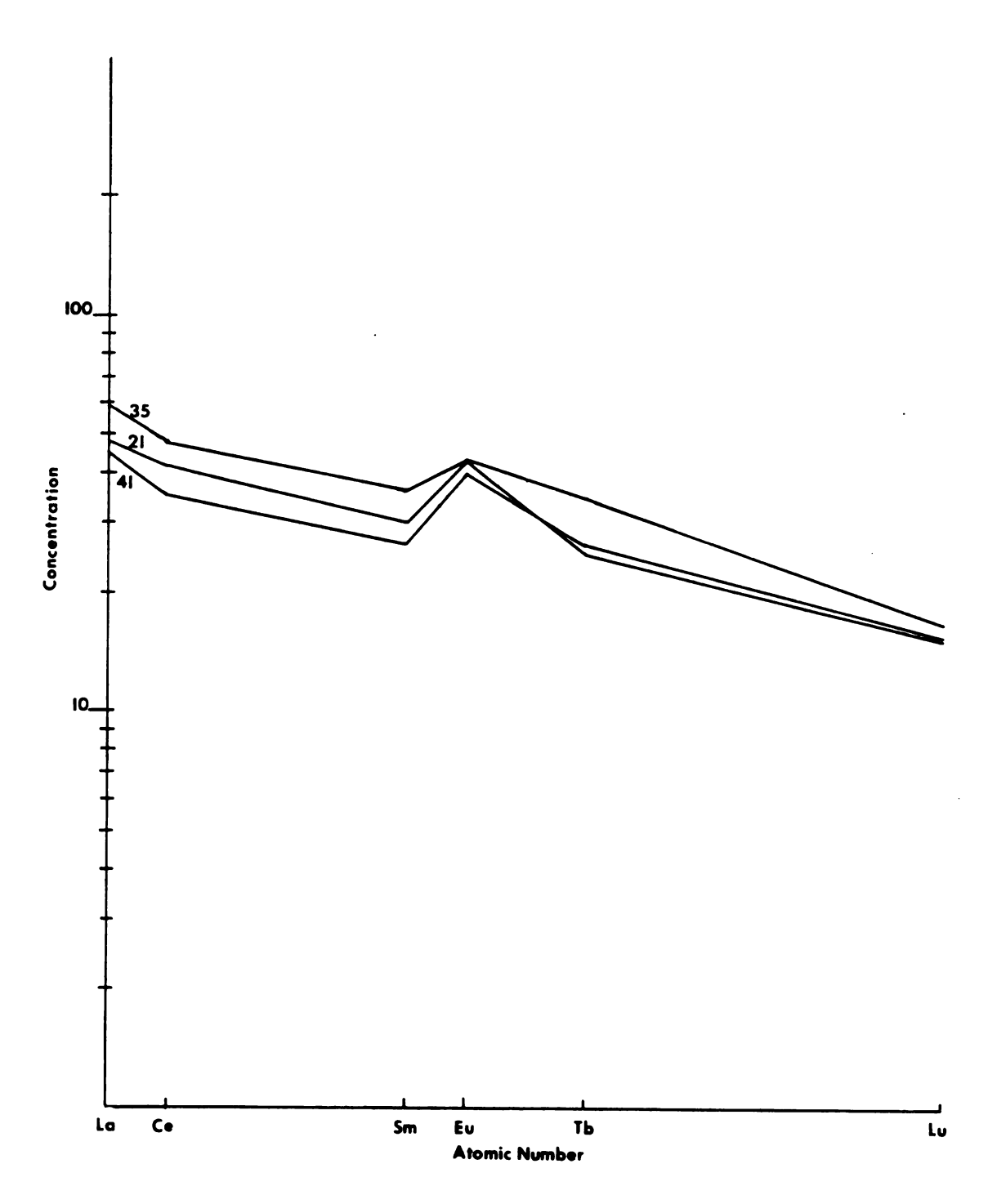


Figure 20: Calculated rare earth element patterns for the gabbro from models in Table 6.

values. The europium anomaly, however, is of the correct size and barium and strontium are moved in the correct directions. It is for just these last two elements, therefore, that different partitioning coefficients must be assumed. The calculated values of P and Ti are higher than those observed, suggestion fractionation of the ilmenite and apatite that commonly occur in these rocks. These minerals are, however, trace element sinks and fractionation of them will only further lower the concentrations. It is more likely that the concentrations of these two elements for the minerals used in the calculations are not accurate.

Despite the inconsistencies just discussed, the preferred model for the origin of the marscoite is the fractionation of minor amounts of plagioclase, olivine, and clinopyroxene from a mixture of the porphyritic ferrodiorite and Marsco epigranite. The porphyritic ferrodiorite itself may be the product of mixing the non-porphyritic ferrodiorite and the Marsco epigranite with some accumulation of plagioclase, olivine, and clinopyroxene.

SUGGESTIONS FOR FURTHER RESEARCH

More research can still be done on the Marscoite suite.

The models proposed in this paper for the origin of the suite should be tested again with detailed mineral analyses and replicate analyses of the Marsco epigranite and the Marsco Summit gabbro. With this data it should also be possible to determine if the ferrodiorites and the marscoite represent a

zoned magma chamber. The role of diffusion should be examined through a petrographic and geochemical study of the contacts within the suite. It would also be interesting to do similar research on the glamaigite, an inhomogeneous hybrid found nearby (Wager et al., 1965; Thompson, 1968).

CONCLUSION

Models considered in this study included mixing, fractionation and combinations of the two. Agreement with the major element data was tested by multiple linear regression analysis. The REE patterns and Ba and Sr values were compared with values calculated from the regression equations. A mixture of the non-porphyritic ferrodiorite and the Marsco epigranite with an accumulation of plagioclase, olivine, and clinopyroxene is the model most consistent with porphyritic ferrodiorite data. Fractionating the same minerals from a mixture of the porphyritic ferrodiorite and Marsco epigranite is most consistent with the marscoite data.

Several conclusions can be drawn, however, even if none of the models presented here are accepted as consistent with the data. First, mixing is the dominant process in the origin of the marscoite, although the simple mixing models proposed by Harker (1904), Wager et al. (1965), and Thompson (1968) are not consistent with the trace element data.

Second, the acidic parent should have a trace element content similar to that of the Marsco epigranite, ie. a small negative Eu anomaly and a high Ba concentration. Third, the ferrodiorites appear to be unrelated to both the Marsco

Summit gabbro and the lavas of the area.

The difficulty in finding a model in agreement with all of the trace element data underscores the fact that we still do not completely understand the behavior of the trace elements during geologic processes such as mixing. This study also illustrates the importance of evaluating data of all types in determining the origin of a specific rock.

BIBLIOGRAPHY

BIBLIOGRAPHY

- Arth, J.G., 1976, Behavior of trace elements during magnatic processes-a summary of theoretical models and their applications: J. Res. USGS, 4, p.41-47.
- Deer, W.A., Howie, R.A., and Zussman, J., 1966, An Introduction to the Rock Forming Minerals. London: Langman. 528pp.
- Donaldson, C.H., Brown, R.W., 1977, Refractory megacrysts and magnesium-rich melt inclusions within spinel in oceanic tholeiites: Indicators of magma-mixing and parental magma composition: Earth Planet. Sci. Lett., 37, p.81-89.
- Eichelberger, J.C., and Gooley, R., 1976, Evolution of silicic magma chambers and their relationship to basaltic volcanism: Los Alamos Scientific Laboratory Report LA-UR 76-1708.
- Exley, R.A., 1980, Microprobe studies of REE-rich accessory minerals: Implications for Skye granite petrogenesis and REE mobility in hydrothermal systems: Earth Planet. Sci. Lett., 48, p.97-110.
- Gamble, J.A., 1979, Some relationships between coexisting granitic and basaltic magmas and the genesis of hybrid rocks in the Tertiary central complex of Sliev Gullion, NE Ireland: J. Volc. Geotherm. Res., 5, p.169-234.
- Gordon, G.E., Randle, K., Goles, G.G., Corlliss, J.B., Beeson, M.H., Oxley, S.S., 1968, Instrumental activation analysis of standard rocks with high-resolution gamma-ray detectors: Geochim. Cosmochim. Acta, 32, p.369-396.
- Harker, A., 1904, Tertiary Igneous Rocks of Skye: Geol. Surv., Scotland Mem., 481pp.
- Hildreth, W., 1981, Gradients in Silicic Magma Chambers: Implications for Lithospheric Magmatism: J. Geophys. Res., 86, p.10153-10192.

- Korotev, R.L., 1978, Geochemical molding of the distribution of rare earth and other elements in a basalt and grain size fraction of soils from the Apollo 17 valley floor and a well tested procedure for accurate instrumental neutron activation analysis of geological materials: Ph.D. Thesis, Univ. of Wisconsin, Madison, 264pp.
- Langmuir, C.H., Vocke, R.D., Hanson, G.N., Hart, S.R., 1978, A general mixing equation with applications to Icelandic basalts: Earth Planet. Sci. Lett., 37, p.380-392.
- Rhodes, J.M., Dungan, M.A., Blanchard, D.P., Long, P.E., 1979, Magma mixing at mid oceanic ridges: Evidence from basalts drilled near 22N on the mid Atlantic ridge: Tectonophysics, 55, p.35-61.
- Taylor, T.R., Vogel, T.A., Wilband, J.T., 1980, The composite dikes at Mt; Desert Island, Maine: An example of coexisting acidic and basic magmas: J. Geol., 88, p.433-444.
- Thompson, R.N., 1980, Askja 1875, Skye 56 MA: Basalt triggered plinian, mixed magma eruptions during the emplacement of the Western Red Hills Granites, Isle of Skye, Scotland: Geol. Rdsch., 69, p.245-262.
- Thompson, R.N., 1968, Tertiary granites and associated rocks of the Marsco area, Isle of Skye: Geol. Soc. Quart. Jour., 124, p.349-385.
- Thompson, R.N., Gibson, I.L., Marriner, G.F., Mattey, D.P., Morrison, M.A., 1980, Trace element evidence of multistage mantle fusion and polybaric fractional crystallization in the Palaeocene lavas of Skye, NW Scotland: J. Petrology, 21, p.265-293.
- Thompson, R.N., Esson, J., Dunham, A.C., 1972, Major element chemical variation in the Eocene lavas of the Isle of Skye, Scotland: J. Petrology, 13, p.219-253.
- Wager, L.R., and Vincent, E.A., 1962, Ferrodiorite from the Isle of Skye: Miner. Mag., 33, p.26-36.
- Wager, L.R., Vincent, E.A., Brown, G.A., Bell, J.D., 1965, Marscoite and related rocks of the Western Red Hills Complex, Isle of Skye: Royal Soc. Phil. Trans., Series A, 257, p.273-307.
- Wood, B.J., and Fraser, D.G., 1976, Elementary thermodynamics for geologists. London: Oxford University Press.
- Wright, T.L., Doherty, P.C., 1970, A linear-programming and least squares computer method for solving petrologic mixing problems: Geol. Soc. Amer. Bull., 81, p.1995-2008.

